Quantum dots in microcavities: from single spins to engineered states of light

Steindl, P.

3 Cross-polarization extinction enhancement and spin-orbit coupling of light for quantum-dot cavity-QED spectroscopy

Resonant laser spectroscopy is essential for the characterization, operation, and manipulation of single quantum systems such as semiconductor quantum dots. The separation of the weak resonance fluorescence from the excitation laser is key for high-quality single- and entangled photon sources. This is often achieved by cross-polarization laser extinction, which is limited by the quality of the optical elements. Recently, it was discovered that Fresnel-reflection birefringence in combination with single-mode filtering counteracting spin-orbit coupling effects enables a three-order of magnitude improvement of polarization extinction [PRX 11, 021007 (2021)]. Here, we demonstrate this method for cross-polarization extinction enhancement in cryogenic confocal microscopy of a resonantly excited semiconductor quantum dot in a birefringent optical micro cavity, and observe a 10× improvement of the single-photon contrast.

This chapter is based on: P. Steindl, J.A. Frey, J. Norman, J.E. Bowers, D. Bouwmeester, W. Löffler, *Cross-polarization extinction enhancement and spin-orbit coupling of light for quantum-dot cavity-QED spectroscopy*, arXiv:2302.05359 (submitted) [101].

3.1 Introduction

Highly pure and indistinguishable single-photon sources [13,15,18,28,57,102,103] and spin manipulation [104] often rely on resonant excitation schemes and require a high degree of polarization extinction of the excitation laser. Such experiments are typically carried out in confocal microscope setups having the required high spatial resolution [105, 106] to address individual quantum emitters, where the excitation beam is directed onto the sample using mirrors and beam splitters. Because all-dielectric (but also metallic) polarization-preserving mirrors [107] do not exist, usually, linearly polarized light with s or p polarization is used, which, due to symmetry and in the plane-wave approximation, is preserved under reflection. Therefore, the maximal polarization extinction ratios (PER) are limited by the quality of available polarizers to typically $10^5 - 10^6$. Now, experimentally, extinction ratios of up to 10^8 [54] have been observed, but the precise origin of this high ratio has only recently been clearly identified. Benelajla et al. [55] found a 3-orders of magnitude PER improvement by mirror-induced pre-compensation of the residual ellipticity of linear polarizers, in combination with single-mode filtering that eliminates detrimental effects caused by spin-orbit coupling at optical reflection [108–110].

Spin-orbit coupling of light leads to angular and spatial beam shift corrections to specular reflection [111, 112], known as Goos–Hänchen [113] and Imbert–Fedorov shifts [114, 115]. The latter effect is also referred to as the optical spin-Hall effect of light [116,117]. Here, both of the elliptical eigenpolarizations [118] experience a small opposite transverse shift which leads to a variation in the degree of the circular polarization over the beam cross-section [119]. Measuring in linear cross-polarization, the unwanted (leaked) polarization component of the beam adopts a Hermit-Gaussian profile [55, 120, 121] with a nodal line in the center, caused by linear polarization projection of the two reflected and shifted beams with opposite helicity. In combination with single-mode fiber detection, Benelajla et al. [55] demonstrated above three orders extinction enhancement after a single optical reflection compared to the bare or conventional polarizer extinction ratio with 90° between the polarizers. This shows a new - only used serendipitously before - application of beam-shifts in addition to high-resolution sensing [122,123] and corrections in astrophysical instruments [124], but the effect has not been clearly identified in confocal microscopy.

Here, we first demonstrate that the elimination of residual scattering from a Glan-type polarizer by propagation or single-mode fiber filtering already enables extinction ratios beyond 10^7, then we investigate the effect of multiple in-plane reflections (under 45° angle of incidence) on the PER. We find that a single Fresnel reflection is optimal, achieving a PER of nearly 10^8. Finally, we demonstrate the PER enhancement effect by reflection in a cryogenic confocal microscope. By careful characterization and optimization of the polarizer rotation angles, we achieve extinction ratios up to 10^7, two orders above the bare polarizer limit, and can clearly attribute this effect to ellipticity and spin-orbit coupling compensation. With this, we demonstrate an improvement of a quantum-dot cavity-QED-based single-photon source.

3.2 Scattering elimination

We start with a simple optical setup shown in the insets of Fig. 3.1. A narrow-linewidth continuous-wave laser with wavelength $\lambda = 935.5\,\mathrm{nm}$ is attenuated with a calibrated set of neutral density filters, mode-filtered with a polarization-maintaining single-mode fiber (PMF) and collimated by an aspheric lens into a Gaussian beam with 0.75 mm beam waist. It is sent to the two polarizers P1 (which is approximately aligned to the incident-light polarization) and P2, which are here two anti-reflection coated calcite Glan-Thompson polarizers, placed 15 cm from each other and mounted in motorized rotation stages with 10^{-2} and 10^{-3} degree resolution, respectively. To analyze the polarizer extinction, the light transmitted through both polarizers is focussed with a lens onto a femtowatt photoreceiver (FWR) that is placed at an adjustable distance d from the analyzer P2, see Fig. 3.1(c). To subtract background light, we use laser modulation and a lock-in amplifier. We determine the polarization extinction ratio $\mathrm{PER} = I_{\mathrm{copol}}/I_{\mathrm{xpol}}$ from the co- and cross-polarized transmitted intensities I_{copol} and I_{xpol}. The front polarizer is kept at a fixed angle β aligned roughly to the polarization of the laser source and I_{xpol} is minimized by rotation of P2.

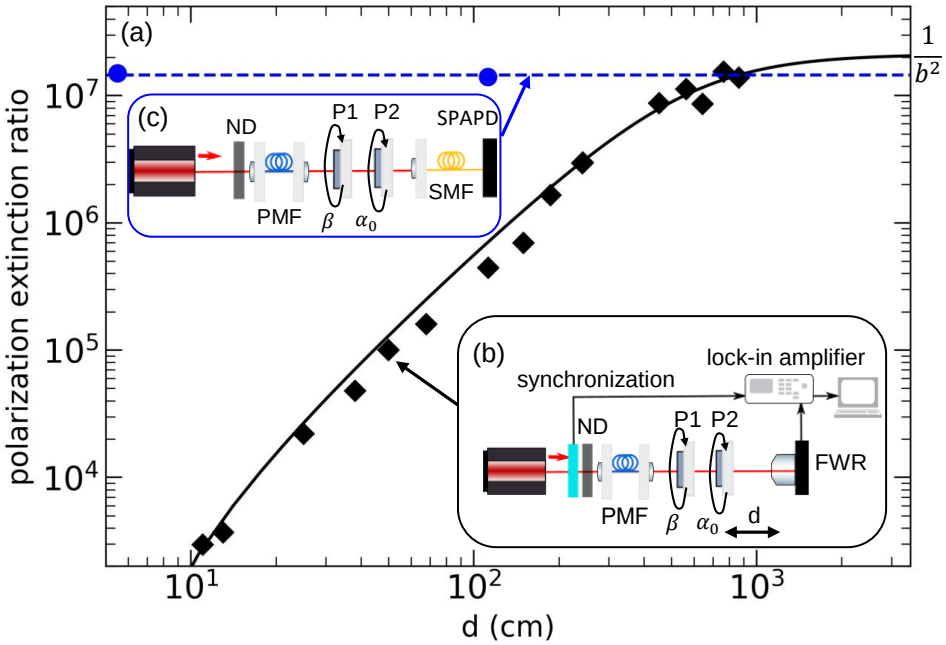

Figure 3.1: The effect of scattered light on the cross-polarization extinction ratio. (a) black symbols: free-space detected PER for increasing detector distance d from the analyzing polarizer, the experimental configuration is sketched in (b). blue: extinction measured using single-mode fiber filtering, (c) shows the setup. The black curve is a model fit as described in the main text.

We measure PER for various distances d up to 8.5 m, collecting in all cases over 90 % of the beam area. The data presented in Fig. 3.1(a) shows a gradual increase of the measured PER with distance, ranging from 10^3 at few centimeter distances to 1.4×10^7 at 8.5 m. Our observed dependency on distance can be explained by scattering including Rayleigh scattering [125]: We model the unwanted light in cross-polarization by (i) residual ellipticity of the polarizers [126] that is limiting the bare extinction ratio to $1/b^2$ [55],

and (ii) (Rayleigh) scattered light, which is quadratically decreasing with distance [127], resulting in $I_{\mathrm{xpol}} = b^2 + b_{\mathrm{scat}}^2/d^2$. We fit our data and obtain $b = (2.1 \pm 0.2) \times 10^{-4}$ and $b_{\mathbf{scat}} = (12.6 \pm 1.2) \times 10^{-5}\,\mathrm{m}^{-1}$, limiting the bare extinction measured after scattering elimination to 2.1×10^7. This value is very close to the extinction of 1.4×10^7 that we achieve by single-mode fiber (SMF) filtering shown in Fig. 3.1(c). We repeat the SMF-filtered experiment at two distances from P2, including at $d = 4.5\,\mathrm{cm}$ where scattering is dominant without fiber filtering, and observe a constant PER. As expected, a single-mode fiber efficiently removes scattered light.

We operate our photodetector close to the dark current limit, and the signal fluctuated by 5% for the highest PERs. Therefore we repeated the experiments with fiber filtering with a fiber-coupled single-photon avalanche photon detector (SPAPD, 25 % detection efficiency, $200\,\mathrm{s}^{-1}$ dark count rate), where the measured PER is limited by dark counts to 6×10^{11}. We obtain a polarization extinction of 1.5×10^7, confirming our previous results. This is more than two orders of magnitude higher than specified. We have also repeated the same experiment with different pairs of the Glan-Thompson polarizers and always found extinction ratios above 10^7. This agrees to earlier studies [125, 126], only surpassed by dedicated studies using 10^{-4} degree resolution rotation stages, resulting in extinction ratios up to $\sim 3 \times 10^9$ [128–130]. In the Appendix 3.6.1, we present additional measurements for various analyzers, and show the effect of the anti-reflection coating of Glan-Thompson polarizers, and compare Glan-Thompson polarizers with nanoparticle polarizers.

3.3 Vector-beam effects upon multiple reflections

Now we investigate the influence of (multiple) in-plane reflections on the achievable polarization extinction ratio using experimental setups with 0, 1, and 2 reflections between the polarizers, as shown schematically in panels (a)–(c) of Fig. 3.2. All mirrors are dielectric thin-film mirrors placed approximately under 45° of incidence, and the last mirror in combination with a translation of the fiber collimation lens is used to optimize coupling into the single-mode fiber, where we achieve a coupling efficiency of 80 % in all cases. The single-mode fiber removes scattered light as investigated in the previous section. The initial beam is approximately s-polarized by P1, both P1 and P2 are Glan-Thompson polarizers. We show similar results for p polarization in the Appendix, Sec. 3.6.2. For each configuration, the polarizer angles α and β are fine-adjusted iteratively around the conventional cross-polarization condition ($|\alpha_0 - \beta| = \pi/2$) to optimize the PER. Note that even a small deviation of about 0.03° from the optimal settings of P1 leads to a reduction of PER by one order of magnitude.

First, we discuss the single-reflection case as shown in Fig. 3.2(b), where we reliably reach an extinction ratio of 6.2×10^7. This extinction ratio is by a factor 3 higher compared to the zero-reflection configuration shown in Fig. 3.2(a). The enhancement is due to compensation of the residual polarizer ellipticities by the small Fresnel-reflection birefringence if the light incident on the mirror is not exactly s or p polarized; and possibly a stress-induced birefringence of the mirror coating. In any case, this birefringence enables for compensation of residual ellipticities of the used polarizers and thus improves the PER [55] compared to the zero-reflection case. As mentioned by Benelajla et al. [55], this can be explained in the plane-wave picture because vector-beam effects and spin-orbit coupling results in higher-order modes, in our case mainly in the first-order Hermite-Gaussian mode [55, 121, 131, 132]. This mode has a nodal line in the center and is shown

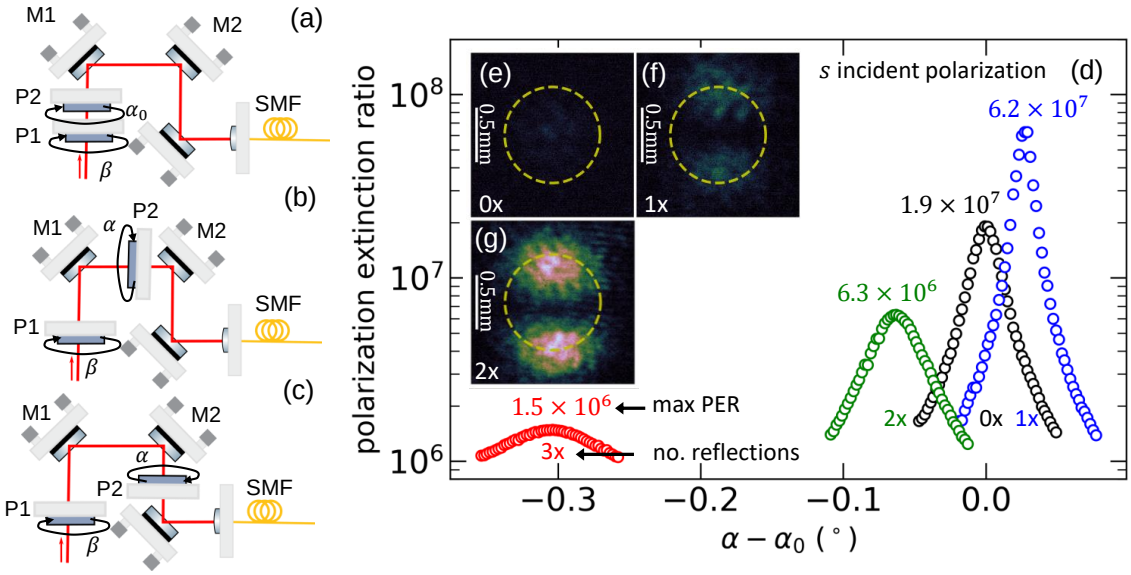

Figure 3.2: Polarization extinction and spin-orbit coupling upon multiple reflections. We use a series of setups with a different number of optical reflections between the polarizers (a-c), determine the maximum achievable polarization extinction (d), and also show the residual unwanted light pattern measured in cross-polarization before coupling into the single-mode fiber (e-g, the dashed circle shows the fiber mode before the collimation lens). In (d), the PER as a function of the analyzing polarizer angle α relative to the conventional cross-polarization angle $\alpha_0 = \beta \pm \pi/2$ is shown. The maximal PER for each configuration with n reflections is indicated.

in Fig. 3.2(f), and it can largely be filtered out by the detection single-mode fiber and does therefore not degrade much the PER.

To further investigate this argument, we have also tested two [Fig. 3.2(c)] and three reflections, each time optimized the polarizer angles, and we observe a reduced PER compared to a single reflection, 6×10^6 after two reflections and 1×10^6 after three reflections. We also observe an increase of the intensity in the first-order Hermite-Gauss mode as shown in Fig. 3.2(g), suggesting that imperfect single-mode filtering can explain the reduction of the PER for multiple reflections.

3.4 Single emitter polarization extinction improvement

Now we investigate whether the method to improve the polarization extinction ratio can also be applied in more complex experimental setups, for which we investigate resonant optical spectroscopy of a single self-assembled InGaAs/GaAs quantum dot (QD) embedded at the antinode of a high-quality micropillar cavity [18,85], using various setups shown in the insets of Fig. 3.3. Instead of the mirror reflection and to independently vary the excitation (P1) and detection polarization (P2), we use a non-polarizing beam splitter (BS) with 90:10 (R:T) splitting ratio to separate excitation and detection paths. The polarization of the excitation narrow-linewidth laser light ($\lambda = 935.5\,\text{nm}$, FWHM = 200 kHz, beam waist 0.75 mm) is controlled with a Glan-Thompson polarizer mounted in a rotation

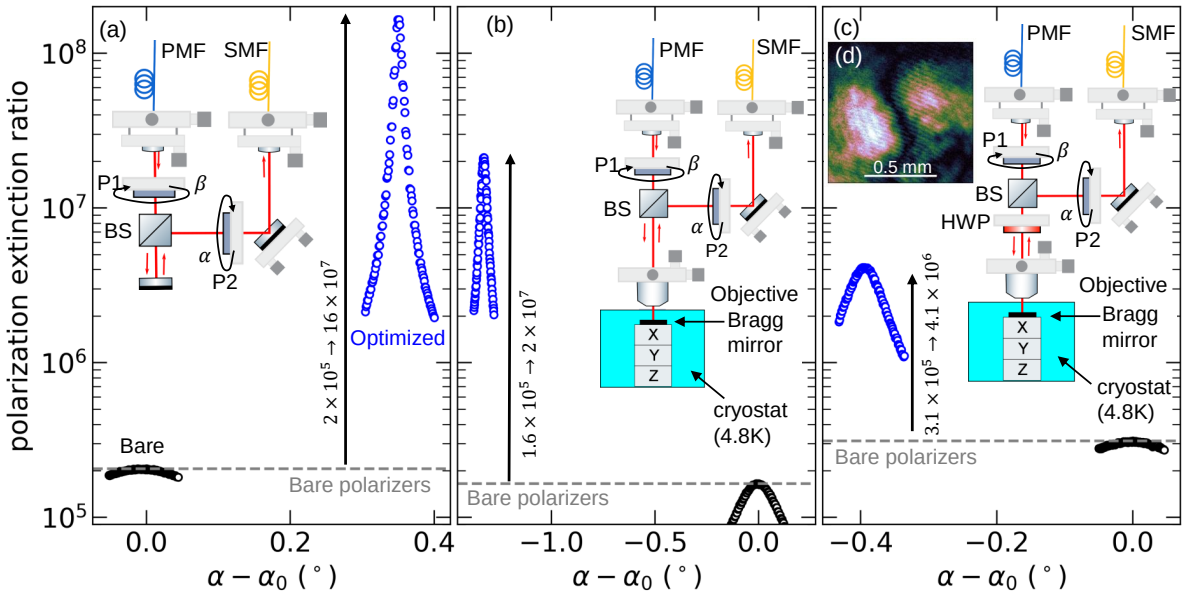

Figure 3.3: Polarization extinction improvement (blue symbols) by reflection in a non-polarizing beam splitter in a cryogenic microscope. Shown is the PER as a function of the angle of the analyzing polarizer α relative to the conventional cross-polarization angle α_0. First, the case is shown where the cryostat is replaced by a flat mirror, where beyond 10^8 improvement is obtained (a). Then the beam is focussed into the cryostat and reflected there and we obtain beyond 10^7 contrast (b). Finally, the case is shown where a half-wave plate is added before the objective in order to align the linearly polarized cavity modes of the device in the cryostat to the polarization frame of the optical setup (c).

stage with an angular resolution of 0.01 deg. The detection polarization selection is done with a nanoparticle polarizer which is less sensitive to alignment, mounted in a 0.001 deg resolution motorized stage; this polarizer has a bare extinction of 1.9×10^5. The transmitted light is coupled into a single-mode fiber (coupling efficiency ~85%) and detected with a SPAPD.

First, we reflect the incident light from a plane dielectric mirror under normal incidence placed below the beam splitter, as sketched in Fig. 3.3(a). We optimize the PER close to s polarization (at the beam splitter) and obtain a PER of 1.6×10^8. This is nearly three orders of magnitude higher compared to bare extinction measured with the nanoparticle polarizer in conventional cross-polarization, reproducing our previous results.

Now, we use a long-working-distance plan apochromat objective (0.4 NA, infinity corrected) focussing the light through two silica glass windows into a close-cycle cryostat cooled to 4.8 K. The light is reflected from the top GaAs/AlAs thin-film Bragg mirror of our quantum dot-cavity device. We repeat the optimization of the polarizer angles which are different due to polarization changes caused by the objective and the two silica windows. As shown in Fig. 3.3(b), even in this complex configuration, we reach an extinction ratio of 2×10^7, a factor 100 above the bare polarization extinction ratio.

Now we perform single-emitter spectroscopy of a single quantum dot in a Fabry-Perot microcavity at around 935.5 nm. The fundamental cavity mode is split by shape and strain induced birefringence [90, 133] by ~ 28 GHz into two orthogonal linearly polarized modes

(V and H). In order to align the polarization frame of reference of the confocal microscope to the frame of the cavity, while avoiding the need to rotate either of them, we use an extra half-waveplate (HWP) below the beam splitter as shown in Fig. 3.3(c). We again optimize the angles of P1 and P2 and reach a PER of 4×10^6 away from the cavity resonances, this is still more than one order of magnitude higher than the bare polarizer extinction ratio. At the same time, as shown in Fig. 3.3(d), we observe in cross-polarization again the typical Hermite-Gauss mode. This suggests that we have demonstrated polarization extinction improvement in a complex cryogenic confocal microscope, despite detrimental effects of the microscope objective and of the focused beam through two cryostat windows, reaching similar extinction ratios as with in-cryostat focussing optics [106].

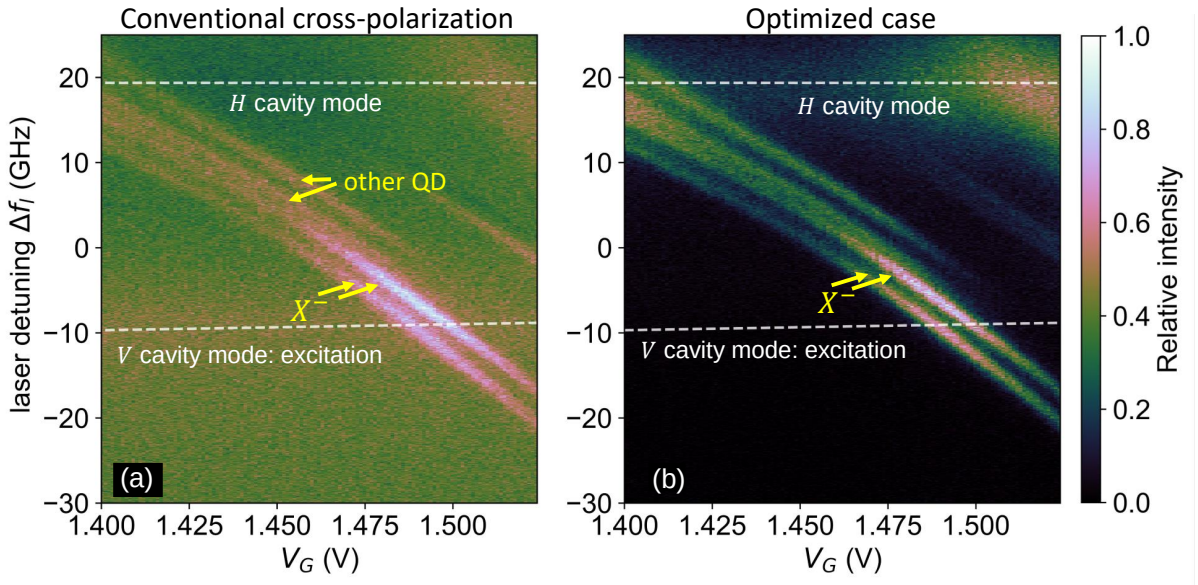

Figure 3.4: Resonant cross-polarized single quantum dot spectroscopy for the conventional cross-polarization configuration (a) and the optimized case (b). Shown is the cross-polarized resonance fluorescence of a negatively charged trion tuned through the cavity resonances by the quantum-confined Stark effect, as a function of laser detuning Δf_l and gate voltage V_G. The incident laser light is polarized along the V cavity axis. Dashed lines indicate both cavity resonance frequencies determined by fits of a semiclassical model [90].

Finally, we demonstrate that the method is also compatible with GHz-scale tuning of the laser, we now show resonant spectroscopy of the negatively charged trion transition X^- of the quantum dot. The dot is embedded in the intrinsic region of a *p-i-n* diode that allows Stark-shift tuning of the quantum dot resonance through the linearly polarized cavity resonances, see Refs. [90, 133]. Under an in-plane (Voigt geometry) magnetic field of 500 mT we observe in Fig. 3.4 the expected transition doublet [98]; each plot shows the normalized single-photon detection rate acquired under an identical excitation configuration. Compared to the conventional cross-polarization condition shown in Fig. 3.4(a) we see a clear improvement by the optimization polarization condition in Fig. 3.4(b). The ratio of the single photons emitted by the quantum dot to background laser light increases from ~2 to ~25 - a significant improvement if used as a single-photon source. Note that both the single-photon purity and also indistinguishability [28] benefit from this improved laser extinction. Additionally, the presented technique can be combined with other meth-

ods used for purity and indistinguishability optimization based on spectral filtering [134], non-resonant excitation [17].

3.5 Conclusions

In conclusion, we have clearly identified the polarization extinction improvement effect by optical reflection and spin-orbit coupling of Benelajla et al. [55] in a complex cryogenic confocal microscope setup and obtained more than one order of magnitude improvement of a quantum-dot based single-photon source. We have shown that single-mode fiber detection is important for the reduction of both unwanted scattered light as well as higher-order modes that appear unavoidably by spin-orbit coupling at the mirror or beam splitter. Only with this mode filtering, the polarization extinction ratio enhancement can be described in a plane-wave picture as a reflection-induced birefringence compensation of the residual elliptical polarization of linear polarizers. We have demonstrated that this extinction enhancement has a direct impact on the single-photon contrast in resonant quantum dot spectroscopy, which we have demonstrated with a single quantum dot in a polarization non-degenerate optical micro cavity. To obtain even higher polarization extinction ratios than those reported here (4×10^6), one should rotate the cavity device and remove the half-wave plate since this wave plate most likely also leads to spin-orbit coupling induced modal changes [135] similar to multiple reflections that we have investigated here.

3.6 Appendix

3.6.1 Scattering elimination with various analyzers

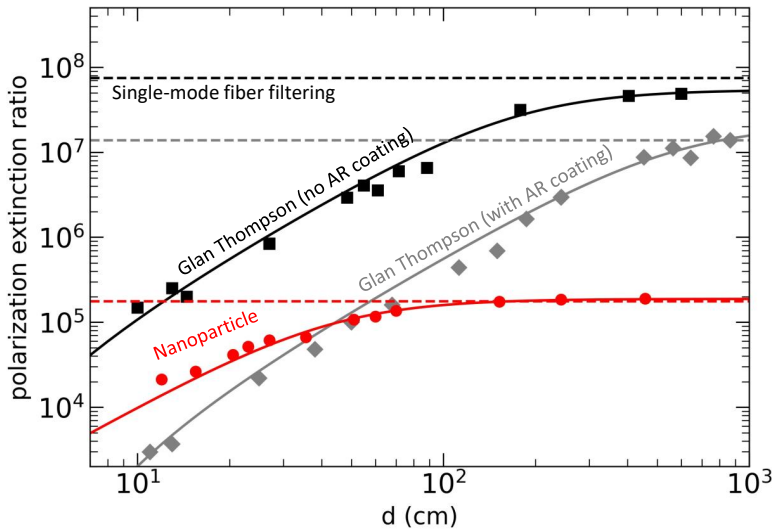

Figure 3.5: Maximum conventional (without mirror reflection) polarization extinction ratio for various analyzer types and conditions: The dashed horizontal lines show the PER using a single-mode fiber, the symbols show the PER using a free-space photo detector at various distances d behind P2. As analyzing polarizer, we used a nanoparticle polarizer (red), and a Glan-Thompson polarizer without (black) and with (gray) anti-reflection coating. Solid lines show the model fit.

In Sec. 3.2 of the main text, we have discussed the importance of the elimination of scattered light for maximal PER. Here we show results (Fig. 3.5) for a wider range of analyzing polarizers P2. We compare Glan-Thompson analyzing polarizers with and without anti-reflection (AR) coating, and a nanoparticle polarizer; the polarizer P1 is an AR-coated Glan-type polarizer in all cases. As in the main text, we model the distance-

Analyzer type	b (10^{-4})	b_{scat} ($10^{-4}\,\mathrm{m}^{-1}$)	Bare extinction $1/b^2$	SMF measured PER
Glan Thompson polarizer (wo AR coating)	1.35 ± 0.03	2.3 ± 0.1	$(5.45 \pm 0.2) \times 10^7$	7.50×10^7
Glan Thompson polarizer (with AR coating)	2.1 ± 0.2	12.6 ± 1.2	$(2.1 \pm 0.3) \times 10^7$	1.38×10^7
Nanoparticle polarizer	23.0 ± 0.3	9.8 ± 0.3	$(1.88 \pm 0.04) \times 10^5$	1.76×10^5

Table 3.1: Fit parameters of the measurements shown in Fig. 3.5.

dependent PER and fit to the data, and we show the fit results of the cross-polarization intensity $I_{\mathrm{xpol}} = b^2 + b_{\mathrm{scat}}^2/d^2$ in Table 3.1. As expected [126], our data shows that AR coating leads to (i) additional scattering captured as an increase in b_{scat} and (ii) extra residual ellipticity of the polarizer reducing the maximal bare extinction. The maximal

bare extinction ratio achieved with the nanoparticle polarizer is strongly reduced, most likely due to residual birefringence of its glass support [126].

3.6.2 Maximal polarization extinction upon multiple reflections

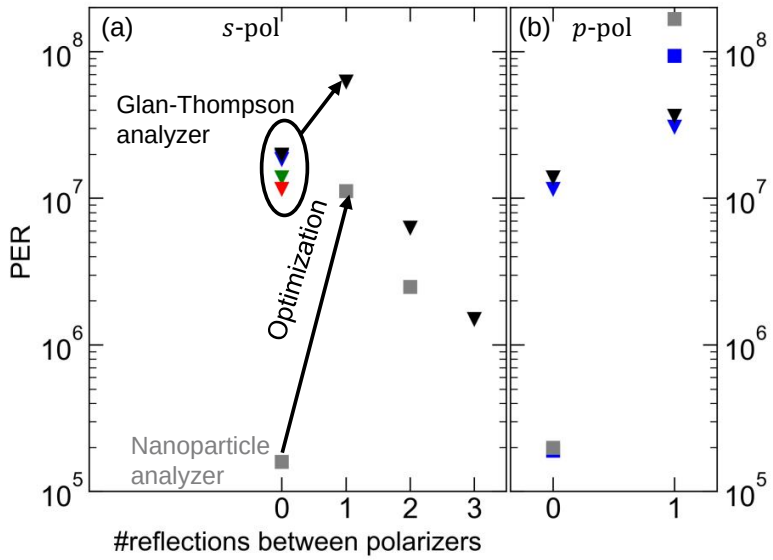

Figure 3.6: Polarization extinction ratio for a different number of reflections for s-polarized (a) and p-polarized (b) incident light, for a Glan-Thompson analyzer (triangles) and a nanoparticle analyzer (squares).

In this section we show additional data for multiple reflections for different polarizer types, and also for s-polarization. As reported by Benelajla et al. [55] and shown in Fig. 3.6, this PER improvement is achieved for both s- and p-polarized light. While the observation of the enhancement is not polarizer-type specific, the absolute value of the maximal PER is a function of the detrimental ellipticity of the polarizers, thus it can vary between individual polarizers.